

A Two-electrode, Double-pulsed Sensor Readout Circuit for Cardiac Troponin I Measurement

Siang-Sin Shan, *Student Member, IEEE*, Shao-Yung Lu, *Student Member, IEEE*, Yuan-Po Yang, Shu-Ping Lin, *Member, IEEE*, Patrick Carey, Minghan Xian, Fan Ren, *Fellow, IEEE*, Stephen Pearton, *Fellow, IEEE*, Chin-Wei Chang, Jenshan Lin, *Fellow, IEEE*, and Yu-Te Liao, *Member, IEEE*

Abstract—This paper presents a pulse-stimulus sensor readout circuit for use in cardiovascular disease examinations. The sensor is based on a gold nanoparticle plate with an antibody post-modification. The proposed system utilizes gated pulses to detect the biomarker Cardiac Troponin I in an ionic solution. The characteristic of the electrostatic double-layer capacitor generated by the analyte is related to the concentration of Cardiac Troponin I in the solvent. After sensing by the transistor, a current-to-frequency converter (I-to-F) and delay-line-based time-to-digital converter (TDC) convert the information into a series of digital codes for further analysis. The design is fabricated in a 0.18- μm standard CMOS process. The chip occupies an area of 0.92 mm² and consumes 125 μW . In the measurements, the proposed circuit achieved a 1.77 Hz/pg-mL sensitivity and 72.43 dB dynamic range.

Keywords—Cardiac Troponin I, current-to-frequency converter, screening effect

I. INTRODUCTION

As a result of the increasing aging population and changing dietary habits, the number of patients with cardiovascular diseases (CVDs), such as coronary syndrome and acute myocardial infarction (AMI), is rapidly increasing. According to a report by the World Health Organization (WHO) in 2016, 31% of deaths worldwide are caused by CVDs. Fortunately, CVDs can be predicted and prevented in the early stage by detecting specific biomarkers in the blood. The concentrations of biomarkers increase before patients feel severe discomfort. Cardiac Troponin I, for example, is a commonly used biomarker that is released into the blood when the myocardium is damaged. Therefore, detecting Cardiac Troponin I is an attractive method to diagnose the condition of patients with CVDs.

Several methods have been proposed for conducting Cardiac Troponin I measurements. As examples, electrochemical sensors can be fabricated using aptamers [1], carbon nanofibers [2], or gold nanoparticles (AuNPs) [3] [4]. Though low detection limits were achieved in these studies, the sensing times are still too long and not suitable for rapid screening. As technology has progressed, bio-sensors have been designed and developed to achieve high sensitivity and a large dynamic range over a wide concentration range of biomarkers for use in diagnosis. Semiconductor-based sensors, such as the ion-sensitive field-effect transistor (ISFET) [5] [6] [7] [8], biologically functionalized field-effect transistor (BioFET) [9], and DNA field-effect transistor (DNAFET) [10], can provide reliable and fast measurements for composition analysis. Currently, the most commonly used method for detecting potential diseases is to test body fluids, such as serum urine and blood, using biochemical

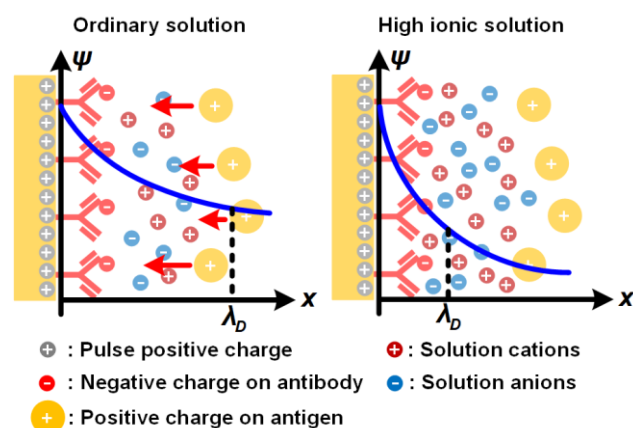


Fig 1. Screening effects under different concentrations.

analysis. However, when the biomarker is in a high-concentration ionic solution, the measurement results may be severely affected by shielding effects, or so-called screening effects [11].

Fig. 1. shows the variation in Debye length, λ_D , in solutions with different ion concentrations. Debye length is defined as the physical distance that an electrical field generated by a charge can act on neighboring charged particles/molecules. As shown in Fig. 1, Debye length becomes shorter as the ionic strength increases. Therefore, in a high ionic concentration solution, the Debye length is small, and thus, fewer particles can be attracted or repulsed, making it difficult for antibodies and antigens to form and generate a stable potential. In addition, an unstable potential is induced by many free antigens at the gate of the FET under high-concentration environments, which leads to a lower sensitivity and unbalanced output current fluctuations [12] [13].

Much research effort has been expended to determine how to measure biomarkers in a highly ionic solution directly. Chu et al. [12] designed an electric-double-layer (EDL) field-effect transistor (FET) using an AlGaIn/GaN high electron mobility transistor (HEMT) and operated it in a linear amplification region. Yang et al. [14] designed a double-layer sensing structure that solves the problem of the maximum distance between the traditional transistor sensor surface and the antibody for effective sensing. With the reduced electrode distance, the potential gradient can be maintained, which provides an electrical field to draw the charged antigen toward the electrode surface. Therefore, antigens beyond the Debye length can still be measured, and the antibody-antigen reaction can be modeled with the Langmuir extension model and spring

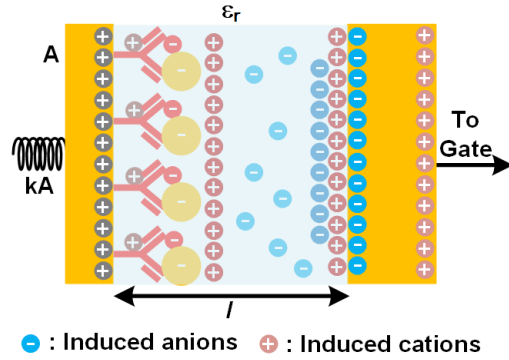


Fig 2. Electric double-layer capacitor model.

model [14]. Distinct from [12], a double-layer sensor architecture adopts a gate electrode separated from the solution to give a stable voltage to the gate of the transistor, performing voltage to current conversion and utilizing charge induction to reduce the screening effect [14]. In addition, this system uses a double-pulsed method at the gate and drain terminals to ensure that the channel charge does not accumulate, and the electrode is reset before measurement. However, both designs require a bulk measurement instrument and wirings. In this work, we present a silicon chip integrated with a CMOS sensing transistor, which can provide an adequate measure of Cardiac Troponin I for assessing the cardiac disease index. The readout circuitry provides a reconfigurable pulse width, amplitude, and recording window length for a wide range of biosensing applications. The design further improves the measurement linearity, sensitivity, and signal-to-noise ratio (SNR) using the time-domain readout technique.

This paper is organized as follows: the sensing mechanism is discussed in Section II, and the architecture of the proposed circuit is described in Section III. Section IV presents the fabrication of the biosensing system and the measurement results. A brief conclusion is addressed in Section V.

II. CONCEPT OF THE SENSING MECHANISM

In electrolytes, Debye length describes the distance at which a charge can act on another charge effectively. Assuming the electrolyte is monovalent and symmetrical, the Debye length can be derived as:

$$\lambda_D = \sqrt{\frac{\varepsilon RT}{2 \times 10^3 F^2 C_0}} \quad (1)$$

where λ_D is Debye length, ε is the dielectric constant of the analyte, R is the gas constant, F is the Faraday constant, T is absolute temperature, and C_0 is electrolyte concentration in molarity (M). From the Gouy-Chapman model, the Debye capacitance density can be derived as:

$$C_{DEBYE} = \frac{\varepsilon}{4\pi\lambda_D} = \frac{1}{4\pi} \sqrt{\frac{2 \times 10^3 F^2 \varepsilon C_0}{RT}} \quad (2)$$

When the pulse is applied to the electrode, the double-layer forms at the solution-electrode interface and creates a double-layer capacitance, which is correlated with the electrolyte concentration (C_0) [15].

In an isolated system where the net plate charge is fixed, the lateral redistribution of the surface charge density coupled to the transverse reorganization of the ionic charge distribution in the electrolyte can cause the EDL capacitance to vary [16]. A relaxing gap capacitor is used in Fig. 2 to model the effects of the varying capacitance. The EDL capacitance varies with charge diffusion in the solution until charge equilibrium is reached. This phenomenon can be further explained by Hooke's Law. Therefore, on a microscopic scale, the electrostatic energy of the capacitor for a fixed surface charge density, d , can be derived as [16]:

$$E(d, l) = \frac{Ad^2 l}{2\varepsilon_r \varepsilon_0} + \frac{kA}{2} (l - l_0)^2 \quad (3)$$

where A is the plate area, l_0 is the initial distance between two plates, and k is the spring constant. By Hooke's Law, spring length is determined by:

$$l = -\frac{\vec{F}}{k} \quad (4)$$

Assuming that the whole system is in the damped simple harmonic motion, l can be derived as:

$$l(t) = l_0 + A_0 e^{-\frac{bt}{m}} \cos(\omega' t + \varphi) \quad (5)$$

where A_0 is the amplitude of the pulse, b is the damping factor of the bulk solution, m is the total mass of charge, and φ is the phase. According to the above equations, in a fixed analyte concentration, the damping time to the steady-state corresponds to the capacitance and conductivity of the solution. The dielectric constant of the solution decreases as the ionic concentration increases. Besides, Debye length is inversely correlated with the ionic concentration, resulting in an increase in EDL capacitance as the conductivity increases. Therefore, the capacitance can be denoted as:

$$C_{EDL} = \frac{2E(d, l)}{V_{pulse}^2} \quad (6)$$

where V_{pulse}^2 is the amplitude of the gate pattern to the sensor. Equation (6) gives the dynamics of the damping effect while the pulse is applied to the sensor and analyte.

On a macroscopic scale, when the electrostatic energy becomes stable in the capacitor, the final DC value of the gate voltage will be determined by the sum of the EDL capacitance and parasitic capacitance, C_{GS} and C_{GD} . Therefore, for different concentrations of analytes, the gate voltage varies because of the capacitive voltage divider. Theoretically, the analytes can be assessed by measuring the voltage pattern at the gate terminal; however, to avoid other charge leakages, the drain current, which is amplified by the current mirror, is recorded in the proposed system.

As observed from the waveform of the sensing electrodes, the analyte information is in the form of the settling response and the stable voltage of the gate terminal. Measuring the voltage in a stable state gives precise results, and the data recorded from the settling response provide substantial gain and kinetic dynamics for the charge reaction between the solution

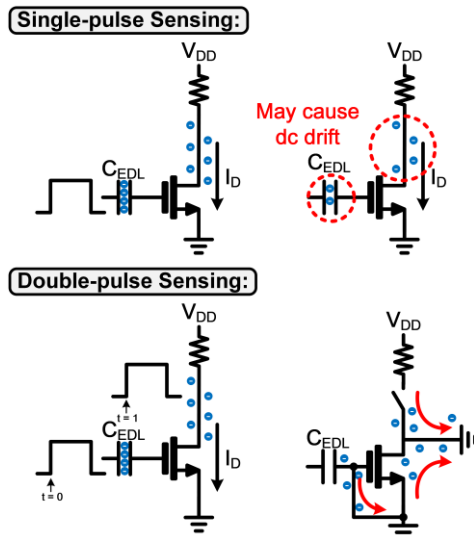


Fig 3. Single-pulse sensing and double-pulse sensing methods.

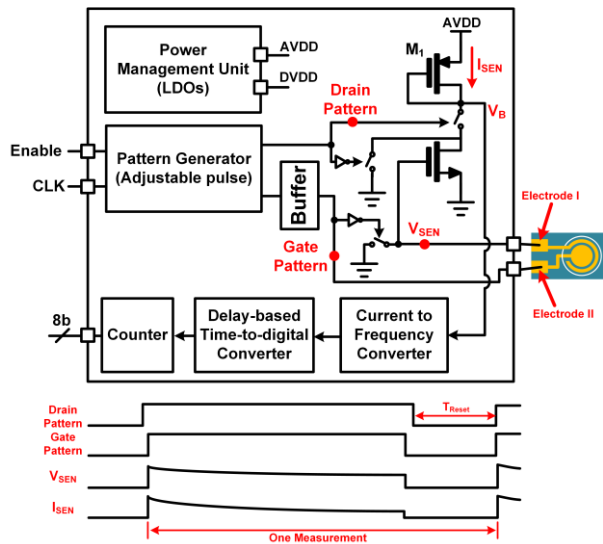


Fig 4. Architecture of the proposed circuit.

and electrode. The circuit for the gated-pulse measurement is presented in the next section

III. PROPOSED READOUT CIRCUIT AND SENSOR ARCHITECTURE

In a conventional single-pulse readout circuit, charges may accumulate on the gate and drain after each measurement because of the floating-gate effect. Fig. 3 shows a conceptual diagram of the charge accumulation. Without resetting the gate, the accumulated charge shifts the gate/drain voltage in each measurement. This work utilizes a double-pulse technique and resets before measurement, which activates the drain and gate paths sequentially to mitigate the charge accumulation at the gate and drain of the sensing transistor.

Fig. 4 shows a block diagram and the output patterns of the proposed readout circuit, mainly including an adjustable pattern generator, a current-to-frequency (I-to-F) converter, and a delay-line-based time-to-digital converter (TDC). The pattern generator is responsible for generating two adjustable duration

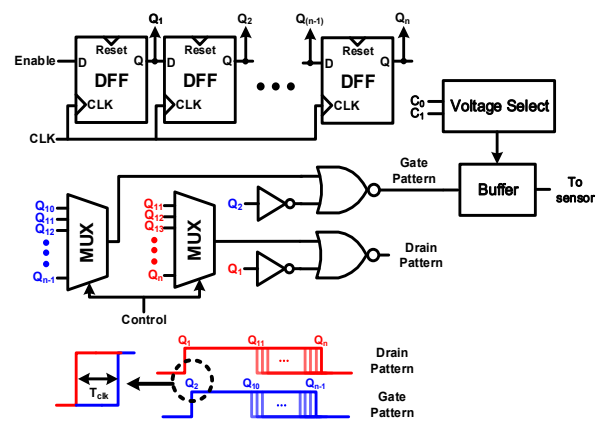


Fig 5. Schematic of the pattern generator.

pulses to the drain and gate of the transistor, which operates as a transconductance device for voltage to current.

As the gate pattern passes the sensor and analyte, V_{sen} varies according to the double-layer capacitance on the electrode-solution interface until the energy stored in the double-layer capacitor remains stable. The corresponding voltage at the gate terminal of the NMOS transistor creates the drain current, I_{sen} , which is injected into the following I-to-F converter. The change in I_{sen} results in a change in the output frequency of the oscillator. Then, a delay-line based TDC converts the I-to-F outputs into digital codes that represent the analyte concentration.

A. Pattern Generator

The reconfigurable pulse delays between the gate and drain patterns are applied to different sensors or different concentrations. For example, when measuring low-concentration troponin I, the response is often long, so an extended pulse signal is needed to provide sufficient time to acquire steady information. For measuring other analytes with a faster response or the dynamics of charging/discharging of the EDL capacitor, the generator can create short pulses to increase the acquisition speed. Fig. 5 shows a schematic of the pattern generator. A programmable shift register controls the delay between the drain and gate patterns. In the generator, one input of each NOR gate is connected to Q_1 and Q_2 of the D-flip-flops, respectively; therefore, a time delay is generated between the rising edge of two clock signals (T_{clk}), which defines the unity time of the acquisition length. For falling edges, two 16-to-1 multiplexers (MUXs) with the same control signal are used. Two MUX inputs are shifted for choosing T_{clk} . For example, when the control bit is 0000, Q_{10} and Q_{11} will be sent to the output; when the control bit is 1111, Q_{n-1} and Q_n will be sent to the output. By this method, a time delay for T_{clk} can be created between two falling edges of the signal. In the design, the drain pattern can be adjusted from $10T_{clk}$ to $(n-1)T_{clk}$, and the gate pattern can be adjusted from $8T_{clk}$ to $(n-3)T_{clk}$, where n is the number of delay cells. $T_{clk} = 0.01$ ms (100 kHz) is adopted in this design. The number (n) of time steps can be selected from 10 to 26, giving different gate pulse widths $((n-2) \times T_{clk} = 80-240\mu s)$. The delay between drain and gate pulses is $2T_{clk}$. Also, the reset signal is controlled by the negative phase of the drain

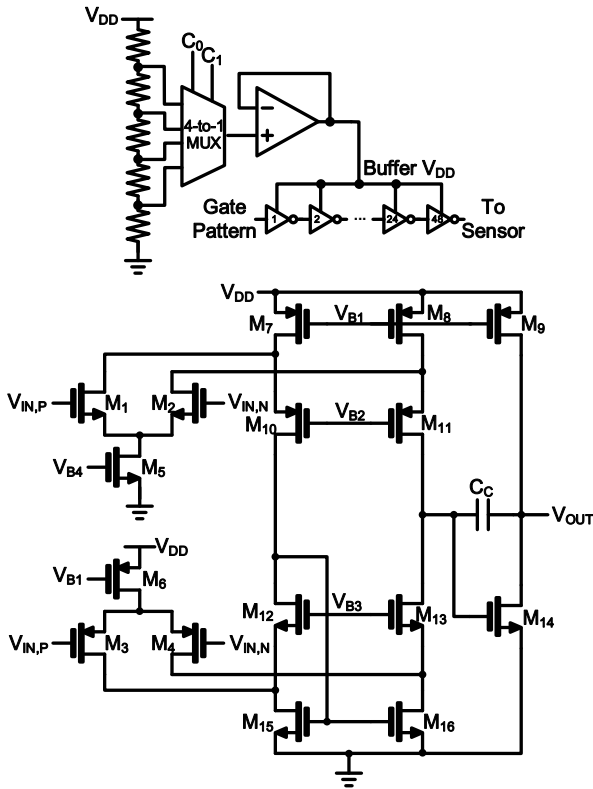


Fig 6. Schematic of the adjustable V_{DD} generator and buffer.

pattern signal. As mentioned above, the length of the gate pattern decides the duration for each measurement. It can be adjusted according to different electrode size/type and response/reaction time.

Moreover, in order to detect various substances, which may have different reaction potentials and adjust the amplification for the signals, the readout circuitry needs to generate an accurate voltage to stimulate the chemical reaction. In the pattern generator, a V_{DD} -adjustable buffer is implemented to adjust the amplitude of the gate pattern. A schematic of the V_{DD} adjustment circuit is shown in Fig. 6. It mainly includes a resistor chain, 4-to-1 MUX, and folded-cascoded differential-to-single-ended amplifier. The resistor chain generates four different voltages, and the output voltage is controlled by two external signals, C_0 and C_1 . To ensure that the amplifier can work over a wide change in voltage, a complementary input stage is employed. The second stage of the amplifier provides extra amplification and voltage swing. To supply enough power for the buffer, the W/L ratio of two transistors (M_9 and M_{14}) in the second stage is about 40X larger than that in the first stage. The output of the unity-gain amplifier is applied to the inverter buffer stages to adjust the pulse amplitude. Considering the threshold voltage of the sensing transistor in the sub-micrometer CMOS process, the pulse voltage is set in a range from 0.5 to 1.1 V to keep the transistor operated in the saturation region. With the adjustable pulse amplitude and interval, the design is suitable for a wide range of sensing applications.

B. Current to Frequency Converter (I-to-F)

Fig. 7 shows a schematic and timing diagram of the I-to-F circuit. The I-to-F circuit consists of two charging/discharging

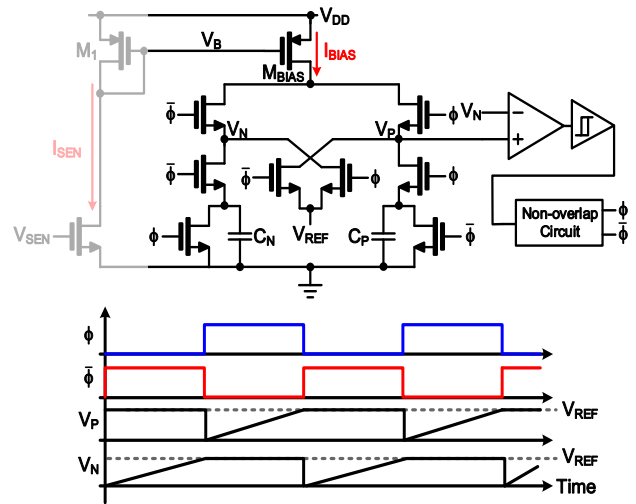


Fig 7. Schematic and timing diagram of I-to-F.

paths, an analog comparator, and a Schmitt-trigger. When ϕ is high, I_{BIAS} starts to charge C_P while C_N starts to discharge, and V_N connects to V_{REF} . As the voltage V_P is charged and becomes higher than V_{REF} , the comparator changes the state, making ϕ change from high to low and swapping the inputs of the comparator. A hysteresis comparator is added to increase the noise margin and avoid metastability. Generally, the comparator offset affects the accuracy of the I-to-F converter. In this structure, the comparator offsets are compensated by swapping the comparator's inputs in the charging and discharging states, resulting in the overall period remaining unchanged [17].

To sense the drain current generated by V_{SEN} , a current mirror is implemented, and this can also prevent the current signal from being directly influenced by the sensing circuit. Therefore, I_{BIAS} can be written as:

$$I_{BIAS} = \alpha I_{SEN} = \alpha \beta (V_{SEN} - V_{th,n})^2 \quad (7)$$

where α is the size ratio between M_1 and M_{BIAS} in Fig. 7, β is the transconductance coefficient, and $V_{th,n}$ is the threshold voltage of the sensing transistor (M_2) in Fig. 4. In order to mitigate the effect of channel length modulation, long channel transistor ($L=10 \mu\text{m}$) is used in M_1 and M_{BIAS} . The duration of the output square wave (T_{output}) can be derived as follows:

$$T_{output} = \frac{(C_N + C_P)V_{REF}}{I_{BIAS}} = \frac{(C_N + C_P)V_{REF}}{\alpha \beta (V_{SEN} - V_{th,n})^2} \quad (8)$$

With the relation between I_{SEN} and T_{output} , the concentration of the analyte can be obtained.

C. Delay-line-based Time-to-digital Converter (TDC)

In the TDC design, the limit of detection for the counter-based TDC is determined by the clock speed, leading to tradeoffs among power, area, and resolution [18]. The delay-line-based TDC has the advantage of first-order noise shaping [18], and the minimum delay time of each block determines the resolution, which benefits from the advanced technology node. Thus, the delay-line TDC can achieve a better resolution,

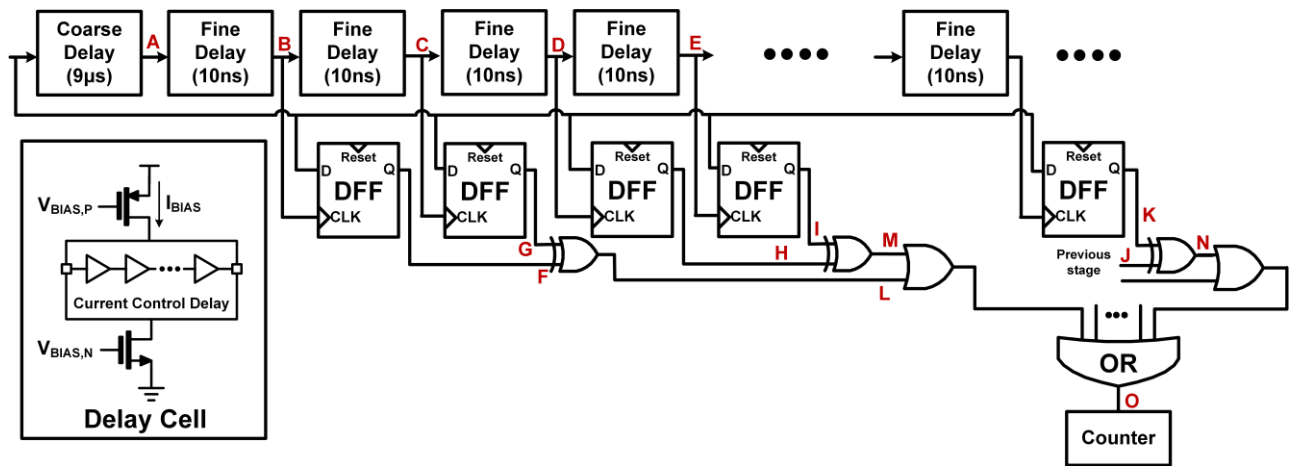


Fig. 8. Schematic of delay-line-based time-to-digital converter with coarse-fine tune.

smaller area, and lower power consumption than the counter-based TDC.

Fig. 8 shows a schematic of the TDC. The delay-line TDC consists of numerous current-starved inverters to create the delay steps. A coarse delay block with a 9- μs delay is employed to reduce the number of bits and silicon area. Afterward, the signal is digitalized by a fine delay chain with a 10-ns delay in each stage, and the total delay is 11.56 μs . The delay of a current-starved delay cell can be adjusted by $V_{\text{BIAS,P/N}}$ to overcome the process variation. To detect the falling edge of the input signal, each clock input of the DFF is connected to the delayed signal, and the sensing signal is connected to the input of the DFF. When the signal has not been delayed for a positive duration, the output of the DFF is pulled from low to high (F, G, H, I, J) sequentially. Every two DFFs share an XOR gate, and the clock signal for the counter is generated (L, M) by implementing the XOR gate to the output signals. When the DFF detects the falling edge of the original signal, the output of the DFF remains at a low level and creates the last clock signal for the counter (N). Finally, the duration of each I-to-F output represents the concentration of the analyte. An 8-bit counter sums the TDC output pulse signals. The counter encodes the duration into a series of digital codes in a binary format.

IV. MEASUREMENT RESULTS

Fig. 9 shows a micrograph of the chip. This chip was fabricated in a 0.18 μm standard CMOS process, and the area is 0.92 mm^2 . To decrease the interference from the environment, the chip is insulated with epoxy after wire bonding. The two-electrode sensor is fabricated using an Au surface and modified with antibodies for troponin I measurement. The sensor and detection chip are assembled on a PCB for functional characterization.

Fig. 10 shows the setup for Cardiac Troponin I measurement. The sensor and chip are mounted to the PCB. The analytes with different concentrations are stored in the fridge before the measurement. When conducting the measurement, a pipette is used for cleaning and change the analytes. The I-to-F output is connected to the digital oscilloscope for continuous readout, and the data acquisition unit analyzes the TDC output.

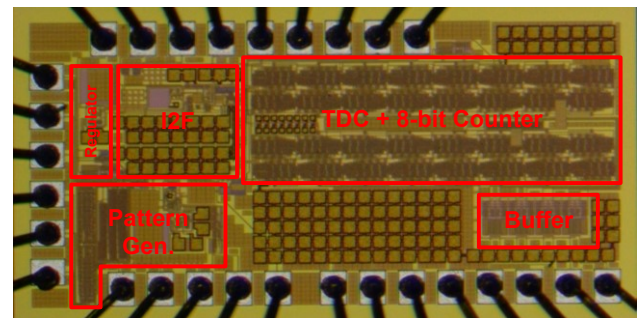


Fig. 9. Chip micrograph.

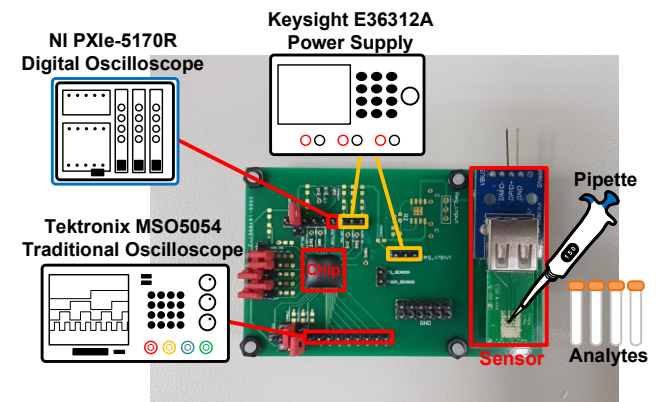


Fig. 10. Measurement setup

A. Sensor Fabrication and Treatment

First, the two electrodes are coated with gold nanoparticles (Vida-Bio, GN3) before post-modification. For surface modification, gold electrodes were treated with ethanol to remove organic contaminants. The self-assembled monolayers were formed by immersing the gold electrodes in an ethanolic 10 mM solution of 12-mercaptopdodecanoic acid (MDA, $\text{C}_{12}\text{H}_{24}\text{O}_2\text{S}$, Sigma-Aldrich) in a sealable container for 18 hours. After that, the MDA-modified gold electrodes were carefully rinsed and cleaned with ethanol and blown dry with a stream of

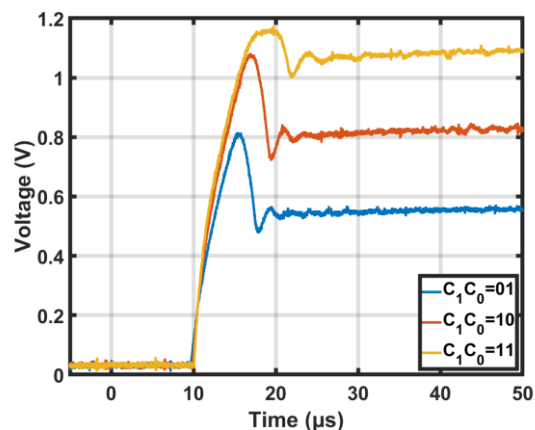


Fig 11. Measurement results of sensor output at different pulse voltage.

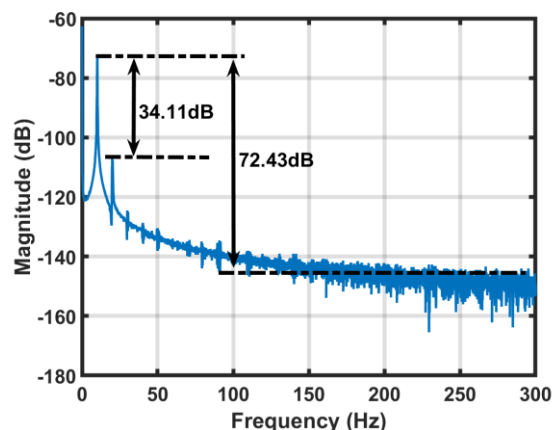


Fig 14. Measurement result of SNR.

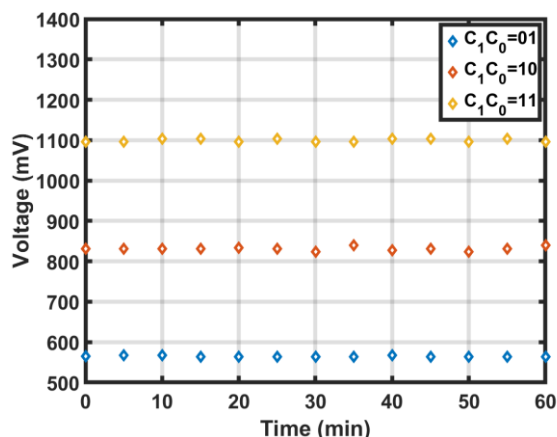


Fig 12. The voltage results for multiple pulsed measurements.

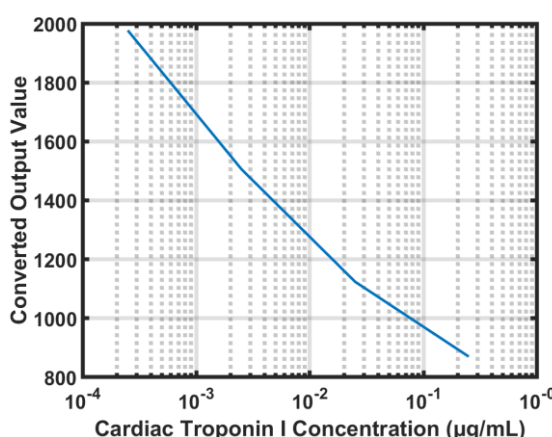


Fig 15. Measurement results of Cardiac Troponin I.

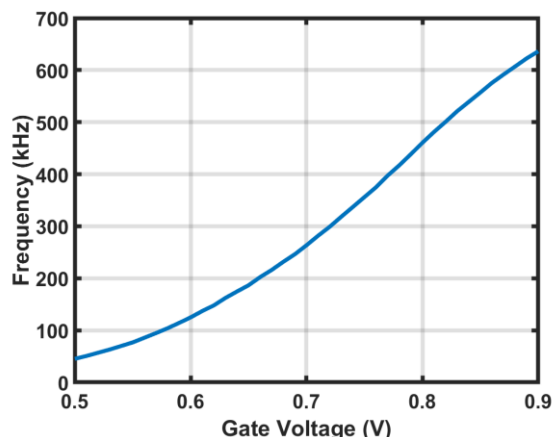


Fig 13. Measurement results of I-to-F output.

nitrogen gas. The MDA-modified gold electrodes were then immersed in an aqueous solution of 10 mg/mL 1-ethyl-3-(3-dimethylaminopropyl) carbodiimide (EDC, Sigma) and 2.5 mg/mL N-hydroxysuccinimide (NHS, Fluka) in citrate buffer solution (pH 5.0) for 1 hour [19]. Then, the MDA-modified gold electrodes were coated with 100 μg/ml Cardiac Troponin I antibody (TnI, GeneTex) for 1 hour to immobilize the TnI on the activated MDA-SAM gold electrodes with chemical bonding.

B. Characterization of the Readout IC

After modification, the sensor was tested with the devised readout IC. Fig. 11 shows the measured results of sensor output with different pulse voltage (adjusted by control bits C_0 and C_1) in a 25ng/mL troponin I solution. The settling response can be observed in this measurement. It takes about 10-20 μs for the three measurements to become stable. Since the EDL capacitance (~nF) is much larger than the parasitic gate capacitance (~pF), and the transistor gate is periodically reset, the residual charge on the gate parasitics does negligible effect on the measurement accuracy. In this design, the maximum gating time is 240μs, the CMOS gate leakage current (tens of fA) only causes tiny voltage droops from the EDL capacitance during measurement. Fig. 12 shows the measured results of multiple pulsed measurements at different voltage levels. The results are captured every 5 minutes in one hour. The good repeatability is observed.

Fig. 13 shows the measurement results of I-to-F outputs. As the gate voltage of the MOSFET changed from 0.5 to 0.9 V, corresponding to 108.28 pg/mL to 356.75 ng/mL from measurement, and V_{REF} was set to 0.6 V, the output frequency changed from 45.2 kHz to 636.2 kHz. The resulting I-to-F sensitivity was 157.68 Hz/nA.

TABLE I
COMPARISON TABLE OF THIS WORK WITH OTHER READOUT MECHANISMS

	[6]	[8]	[7]	[5]	This work
Analyte	Bacteria metabolism (<i>E. coli</i>)	pH	Bacteria metabolism (<i>E. coli</i>)	pH Temperature	Cardiac Troponin I
Sensor Specification	CMOS-Based 4.4 μm x 4.4 μm	Ta ₂ O ₅ 2 μm x 2 μm	Si ₃ N ₄ 50 μm x 50 μm	CMOS-Based 40 μm x 40 μm	Au(External) ϕ:5.2 mm
Detection Method	pH→Voltage	pH→Voltage	pH→Voltage	pH→Duty cycle Temp. → Freq.	Double-pulse concentration→Freq.
Readout Method	pH-TVC ¹	3T-pixel + comparator + DAC	Switched-capacitor Amplifier + SAR ADC	OTA + Sawtooth oscillator	I-to-F + TDC
Sensitivity	33.2 mV/pH	55 mV/pH	30 mV/pH	11.8 mV/pH 3.41 kHz/°C	1.77 Hz/pg-mL
Dynamic Range (dB)	59	41.3	60 and 58.3	44.8	72.43 34.11 (2nd harmonics)
Supply (V)	1.2	3.3	1.8	1.8	1.2
Power (μW)	6500	271000	920	1190	124.78
Tech. (nm)	65	150	180	180	180
Area (mm ²)	25	27.04	3.4	3.6	0.92

¹ pH-to-time-to-voltage conversion

TABLE II
COMPARISON TABLE OF THIS WORK WITH OTHER WORKS ON CARDIAC TROPONIN I

	[1]	[2]	[3]	[4]	This work
Sensor Specification	Aptamer	Carbon nanofiber	AuNP ¹ : Ru-peptide	AuNP	AuNP
Sensing Method	Electrochemical	Electrochemical	Electrochemical	Electrochemical	Electrochemical
Sensing Time(s)	300	N/A	10	3600	80-240 μs
Detection Limit (pg/mL)	1190	200	0.4	200	59.76

¹ AuNP: Gold nanoparticle

Fig. 14 shows the measured spectrum of the whole readout circuitry at a 10 Hz sinusoidal input. The spectrum shows the FFT results that were reassembled from the TDC output digital codes by Matlab. The second-harmonics (HD2) was 34.11 dB, and the dynamic range was 72.43 dB. The HD2 mainly results from V-to-I conversion using the common-source transistor and can be removed by using differential sensing architecture or other linearization methods in the future design.

Fig. 15 shows the measurement results of Cardiac Troponin I while the readout chip was connected with the modified electrode. Between each measurement of different concentrations of the analyte, the sensor was rinsed with de-ionized water and dried with pure nitrogen for 10 seconds. Then, the troponin I analyte was added to the sensor using a mechanically controlled syringe. The converted output value of the stable state in each measurement (one pulse) was recorded by a programmed data acquisition unit. This figure shows the converted values at 160 μs after the pulse was triggered in each measurement. The troponin I concentration range of 250 pg/mL to 250 ng/mL is measured using the readout IC whose power consumption is 124.8 μW at 1.2 V. The resulting sensitivity of the proposed system was 1.77 Hz/pg-mL at a pulse amplitude of 0.6 V, and the duration is 80 μs . From the SNR and sensitivity of the readout circuit, the detection limit of 59.76 pg/mL is achieved. Generally, in cases of acute coronary syndrome, the peak concentration of Cardiac Troponin I can reach 0.3–0.5 ng/mL, which is 10–17 times higher than the 99th percentile of the upper limit of the normal reference population [20] [21]. Thus, this design makes it possible to detect troponin I quickly and conveniently with minimal power consumption.

Table I shows the performance and comparison to the other works. In this study, by taking ISFET as the reference, we developed a sensor readout circuit with a double-pulse mechanism that is suitable for a variety of sensors. Furthermore, we implemented a readout method that mainly uses digital circuits, which not only increases the noise tolerance but also prevents from being affected by non-ideal effects on the amplifier. Table II shows the comparison of our work with other works on Cardiac Troponin I measurements [22]. Because of the advantages of the proposed sensing mechanism, the sensing time is significantly lower, and there is a reduction in the charge accumulation effects. In this study, we developed a rapid readout mechanism. The detection limit can be as low as 59.76 pg/mL. In the future, the circuit and electrode designs can be further improved to measure lower troponin-I concentration detection.

V. CONCLUSION

This paper presents a double-pulsed readout circuit for monitoring Cardiac Troponin I. The double-pulse method can reduce the charge accumulation on the channel of the sensing transistor. The signals are generated from a reconfigurable pattern generator. In addition, with the timing interval between two pulses, the sensing path can be reset, reducing charge accumulation on the drain current path and the sensor. When the pulse is applied to the electrode, different concentrations of the analyte induce changes in the gate voltage and the drain current of the transistor. The current information is then be converted by an I-to-F converter and a delay-line-based TDC. The measurements show a sensitivity of 1.77 Hz/pg-mL with 72.43 dB SNR while only consuming 124 μW at a 1.2-V supply.

VI. ACKNOWLEDGMENT

The authors would like to thank Vida Bio-Technology for supporting sensor information.

REFERENCES

- [1] S. H. Jiang, T. Fan, L. J. Liu, Y. Chen, X. Q. Zhang, Z. L. Sha, Y. L. Liu, J. K. Zhang, "The Detection of cTn I by The Aptamer Biosensor," *Progress in Biochemistry and Physics*, vol. 41, no. 9, pp. 916-920, 2014.
- [2] A. Periyakaruppan, R. P. Gandhiraman, M. Meyyappan, J. E. Koehne, "Label-Free Detection of Cardiac Troponin I Using Carbon Nanofiber Based Nanoelectrode Arrays," *Analytical Chemistry*, vol. 85, no. 8, pp. 3858-3863, 2013.
- [3] M. Shan, M. Li, X. Y. Qiu, H. L. Qi, Q. Gao, C. X. Zhang, "Sensitive Electrogenerated Chemiluminescence Peptide-based Biosensor for the Determination of Troponin I with Gold Nanoparticles Amplification," *Gold Bulletin*, vol. 47, no. 1-2, pp. 57-64, 2014.
- [4] V. Bhalla, S. Carrara, P. Sharma, Y. Nangia, C. R. Suri, "Gold Nanoparticles Mediated Label-Free Capacitance Detection of Cardiac Troponin I," *Sensors and Actuators B: Chemical*, vol. 161, no. 1, pp. 761-768, 2012.
- [5] M. Cacho-Soblechero, K. Malpartida-Cardenas, C. Cicatiello, J. Rodriguez-Manzano and P. Georgiou, "A Dual-Sensing Thermo-Chemical ISFET Array for DNA-Based Diagnostics," in *IEEE Transactions on Biomedical Circuits and Systems*, vol. 14, no. 3, pp. 477-489, June 2020.
- [6] Y. Jiang et al., "A High-Sensitivity Potentiometric 65-nm CMOS ISFET Sensor for Rapid *E. coli* Screening," in *IEEE Transactions on Biomedical Circuits and Systems*, vol. 12, no. 2, pp. 402-415, April 2018.
- [7] M. Duan, X. Zhong, J. Xu, Y. Lee and A. Bermak, "A High Offset Distribution Tolerance High Resolution ISFET Array With Auto-Compensation for Long-Term Bacterial Metabolism Monitoring," in *IEEE Transactions on Biomedical Circuits and Systems*, vol. 14, no. 3, pp. 463-476, June 2020.
- [8] Y. Lee et al., "High-Density 2- μ m-Pitch pH Image Sensor With High-Speed Operation up to 1933 fps," in *IEEE Transactions on Biomedical Circuits and Systems*, vol. 13, no. 2, pp. 352-363, April 2019.
- [9] L. Wang, P. Estrela, E. Huq, P. Li, S. Thomas, P. K. Ferrigno, D. Paul, P. Adkin, P. Migliorato, "Fabrication of BioFET linear array for detection of protein interactions," *Microelectronic Engineering*, vol. 87, no. 5-8, pp. 753-755, 2010.
- [10] B. G. Park, S. W. Hwang, Y. J. Park, "MOSFET as a Molecular Sensor," in *Nanoelectronic Devices*, 1st ed., CRC Press, 2012, ch. 7, pp. 363-365.
- [11] V. Adibnia, B. R. Shrestha, M. Mirbagheri, F. Murschel, G. D. Crescenzo, X. Banquy, "Electrostatic Screening Length in "Soft" Electrolyte Solutions," *ACS Macro Letters*, vol. 8, no. 8, pp. 1017-1021, 2019.
- [12] C. H. Chu et al., "Beyond the Debye length in high ionic strength solution: direct protein detection with field-effect transistors (FETs) in human serum," *Scientific Reports*, vol. 7, no. 1, pp. 1-15, 2017.
- [13] C. S. Li et al. "Ion-sensitive field-effect transistor for biological sensing," *Sensors*, vol. 9, no. 9, pp. 7111-7131, 2009.
- [14] J. C. Yang, P. Carey, F. Ren, M. A. Mastro, K. Beers, S. J. Pearton, I. I. Kravchenko, "Zika virus detection using antibody-immobilized disposable cover glass and AlGaIn/GaN high electron mobility transistors," *Applied Physics Letters*, vol. 113, no. 3, 2018.
- [15] S. Venkat, W. John, "Studies on the Capacitance of Nickel Oxide Films: Effect of Heating Temperature and Electrolyte Concentration," *Journal of The Electrochemical Society*, vol. 147, no. 3, pp. 880, 2000.
- [16] M. B. Partenskii, P. C. Jordan, "Relaxing gap capacitor models of electrified interfaces," *American Journal of Physics*, vol. 79, no. 1, pp. 103-110, 2011.
- [17] A. Paidimarri, D. Griffith, A. Wang, G. Burra and A. P. Chandrakasan, "An RC Oscillator With Comparator Offset Cancellation," in *IEEE Journal of Solid-State Circuits*, vol. 51, no. 8, pp. 1866-1877, Aug. 2016.
- [18] S. Henzler, *Time-to-Digital Converters*. Netherlands: Springer Netherlands, 2010.

- [19] S. P. Lin, J. J. J. Chen, J. D. Liao, S. F. Tzeng, "Characterization of surface modification on microelectrode arrays for in vitro cell culture," *Biomedical Microdevices*, vol. 10, no. 1, pp. 99-111, 2008.
- [20] The Writing Group of 2018 Taiwan Guidelines for the Management of Non ST-segment Elevation Acute Coronary Syndrome 2018, "2018 Guidelines of the Taiwan Society of Cardiology, Taiwan Society of Emergency Medicine and Taiwan Society of Cardiovascular Interventions for the management of non ST-segment elevation acute coronary syndrome," *Journal of the Formosan Medical Association*, vol. 117, no. 9, pp. 766-790, 2018.
- [21] V. S. Mahajan, P. Jarolim, "How to Interpret Elevated Cardiac Troponin Levels," *Circulation*, vol. 124, no. 21, pp. 2350-2354, 2011.
- [22] X. Han, S. Li, Z. Peng, A. M. Othman, R. Leblanc, "Recent Development of Cardiac Troponin I Detection," *ACS Sensors*, vol. 1, no. 2, pp. 106-114, 2016.



Siang-Sin Shan received the B.S. degree in Department of Electrical and Computer Engineering at National Chiao Tung University, Hsinchu, Taiwan, in 2019.

Currently, he is working on his M.S. degree in Institute of Electrical and Computer Engineering at National Chiao Tung University. His research is mainly focused on sensor readout frontend and biomedical stimulation circuits.



Shao-Yung Lu received the B.S degree in electrical engineering from National Chiao-Tung University, Hsinchu, Taiwan, in 2015. He is currently working toward the Ph.D. degree in the Department of Electrical and Computer Engineering at National Chiao-Tung University, Hsinchu, Taiwan. His research interests are the design of low power analog integrated circuits, RC oscillator, biomedical circuits and ventilator systems.



Yuan-Po Yang obtained the Doctor of Medicine from Taipei Medical University in 2007. He worked as resident doctor at Mackay Memorial Hospital (2008-2009). In 2010, he completed a fellowship in cardiothoracic surgery, and then he works as an attending physician at Changhua Christian Hospital until now. He also worked at Kikuna Memorial Hospital in Japan in 2013 and focused on echo-guide intravascular intervention. He has published papers in the renowned journals, such as *Acta Cardiologica Sinica (ACS)*, *Journal of Stroke and Cerebrovascular Diseases*, etc.



Shu-Ping Lin obtained her Ph.D. in Biomedical Engineering from National Cheng Kung University in 2008. She was a visiting research associate in Dr. Themis Kyriakides's laboratory at Yale University from 2006 to 2007. She worked as a postdoctoral researcher at the Institute of Atomic and Molecular Sciences, Academia Sinica (2008-2009), and an independent researcher at Industrial Technology Research Institute (2009-2010). In 2010, she joined Graduate Institute of Biomedical Engineering, National Chung Hsing University, as an assistant professor. She was promoted

as an associate professor in 2016. She has published papers in reputed journals, such as NanoToday, Biomaterials, ACS Applied Materials & Interfaces, Biomacromolecules, PLoS ONE, Sensors and Actuators A-Physical, Biomedical Microdevices, Sensors, and Microsurgery, etc. Her present research activities are mainly directed toward designing and developing biocompatible nano/micro biosensors, cell/tissue engineering, electrophysiological measurements, biocompatible and surface functional modification, and neuronal interfaces.



Patrick H. Carey IV is a Graduate Student Fellow with the Department of Chemical Engineering, University of Florida, Gainesville, FL, USA. His research interests include fabrication and characterization of compound semiconductors, along with fabrication of antibacterial coatings for dental implants.



Minghan Xian is a graduate student with the Department of Chemical Engineering at the University of Florida, Gainesville, FL, USA. His research interests include the fabrication and characterization of biosensors and compound semiconductor devices.



Fan Ren is Distinguished Professor of Chemical Engineering at the University of Florida, Gainesville, FL, USA. He joined UF in 1997 after 12 years as a Member of Technical Staff at AT&T Bell Laboratories, where he was responsible for high speed compound semiconductor device development. He is a Fellow of AIChE, ECS, IEEE, APS, MRS and AVS. He was the recipient of the Gordon Moore award from ECS and the Albert Nerken award from AVS.



Steve Pearton is Distinguished Professor and Alumni Chair of Materials Science and Engineering at the University of Florida, Gainesville, FL, USA. He has a Ph.D in Physics from the University of Tasmania and was a postdoc at UC Berkeley prior to working at AT&T Bell Laboratories in 1994-2004. His interests are in the electronic and optical properties of semiconductors. He is a Fellow of the IEEE, AVS, ECS, TMS, MRS, SPIE and APS. He was the recipient of the J.J. Ebers Award from IEEE, Gordon Moore

Award from ECS, John Thornton award from AVS, Adler award from APS and the Bardeen award from TMS.



Chin-Wei Chang received his B.S.(2013) in physics from National Tsing-Hua Univ., ROC and M.S.(2015) in communication engineering from National Chiao Tung Univ., ROC. He is currently a Ph.D. student in electrical engineering at University of Florida where his research focuses on wireless power transfer and biosensing.



Jenshan Lin (S'91-M'94-SM'00-F'10) received the Ph.D. degree in electrical engineering from the University of California at Los Angeles, Los Angeles, CA, USA, in 1994.

From 1994 to 2001, he was with Bell Labs, Murray Hill, NJ, USA. From 2001 to 2003, he was with Agere Systems, Holmdel, NJ, USA. In 2003, he joined the University of Florida, Gainesville, FL, USA, where he is currently a Professor. From 2016 to 2020, he served as a Program Director of the U.S. National Science Foundation, managing the Communications, Circuits, and Sensing Systems Program and several other cross-cutting programs involving wireless, spectrum, semiconductor, security, and machine learning. He has authored or co-authored over 290 technical publications in refereed journals and conference proceedings. He holds 20 U.S. patents. His current research interests include sensors and biomedical applications of microwave and millimeter-wave technologies, wireless power transfers, and other wireless technologies.

Dr. Lin was a recipient of the 1994 UCLA Outstanding Ph.D. Award, the 1997 Eta Kappa Nu Outstanding Young Electrical Engineer Honorable Mention Award, the 2007 IEEE Microwave Theory and Techniques Society N. Walter Cox Award, the 2015 IEEE Wireless Power Transfer Conference Best Paper Award, the 2016 Distinguished Alumnus Award from National Chiao Tung University, Hsinchu, Taiwan, and the 2016 IEEE RFIC Symposium Tina Quach Outstanding Service Award. He was the General Chair of the 2008 RFIC Symposium, the Technical Program Chair of the 2009 Radio and Wireless Symposium, and the General Co-Chair of the 2012 Asia-Pacific Microwave Conference. He will be the Chair of the 2021 Wireless Power Transfer Conference. He served as the Editor-in-Chief of the IEEE TRANSACTIONS ON MICROWAVE THEORY AND TECHNIQUES from 2014 to 2016.



Yu-Te Liao (S'03, M'11) received the B.S. degree in electrical engineering from National Cheng Kung University, Tainan, Taiwan, in 2003, the M.S. degree in Electronics Engineering from National Taiwan University, Taipei, Taiwan, in 2005, and the Ph.D. degree in electrical engineering from the University of Washington, Seattle, in 2011. In August 2011, he joined the Electrical Engineering Department, National Chung Cheng University, Chiayi, Taiwan, as an Assistant Professor. Currently, he is an Associate

Professor at the Department of Electrical and Computer Engineering, National Chiao Tung University. He is the co-recipient of the Best Paper Award of IEEE VLSI-DAT Conference, 2019. His research interests are the design of low power RF integrated circuits, integrated sensors, and biomedical circuits and systems. He is an Associate Editor of IEEE Sensors Journal since 2017.